BIOCHEMISTRY
including biophysical chemistry & molecular biology

Article

pubs.acs.org/biochemistry

Cytotoxic Amphiphiles and Phosphoinositides Bind to Two Discrete Sites on the Akt1 PH Domain

Cheryl S. Gradziel,[†] Yanling Wang,[†] Boguslaw Stec,[†] Alfred G. Redfield,[‡] and Mary F. Roberts*[,†]

[†]Department of Chemistry, Boston College, Chestnut Hill, Massachusetts 02467, United States

[‡]Life Sciences, Brandeis University, Waltham, Massachusetts 02454, United States

ABSTRACT: The mechanism of binding of two promising anticancer agents (the cytotoxic alkylphospholipids perifosine and miltefosine) to the Akt PH domain is investigated by high-resolution field-cycling ^{31}P nuclear magnetic resonance (NMR) spectroscopy using a spin-labeled recombinant PH domain. These results strongly indicate that there are two discrete amphiphile binding sites on the domain: (i) the cationic site that binds phosphoinositides and some alkylphospholipids and (ii) a second site that is occupied by only the alkylphospholipids. The identification of this second site for amphiphiles on the Akt1 PH domain provides a new target for drug development as well as insights into the regulation of the activity of the intact Akt1 protein. The field-cycling NMR methodology could be used to define discrete phospholipid or amphiphile binding sites on a wide variety of peripheral membrane proteins.

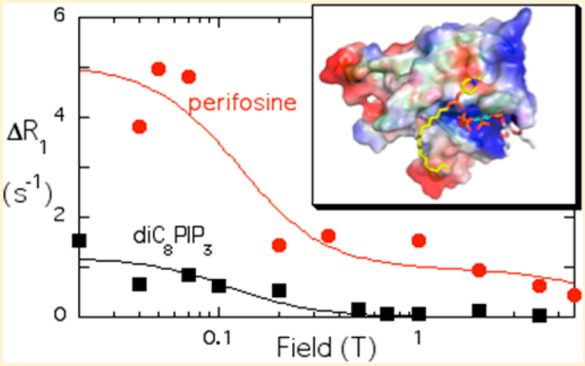

The PI3K/Akt pathway regulates cell survival and growth and is often activated in many varieties of cancer.[1] PI3K, phosphatidylinositol-3-phosphate kinase, generates phosphatidylinositol 3,4,5-triphosphate (PIP_3), a second messenger for enhanced cell growth. Akt (also called protein kinase B) is a cytosolic protein that is transiently anchored on the plasma membrane when its PH domain binds to PIP_3. Crystal structures of its separately expressed PH domain with inositol 1,3,4,5-tetraphosphate have been determined;[2,3] these identify a cationic site on the surface of the domain that binds the phosphorylated inositol moiety. It is postulated that upon phosphorylation of Akt by several other kinases (such as PDK1, PKA, or mTORC2), the enzyme is released from the membrane and, in this activated state, phosphorylates a large number of cytosolic targets, with the net result a sending survival and growth signals into the nucleus. In cancer cells, Akt activation is often dysregulated.[1]

Alkylphospholipids or ALPs are single-chain amphiphilic molecules that have been shown to reduce the level of Akt membrane localization upon cell stimulation.[4,5] If Akt is not transiently located at the membrane, it cannot be appropriately phosphorylated, and its ability to phosphorylate targets is dramatically reduced. Both miltefosine and perifosine are zwitterionic ALPs that hold promise as anticancer therapeutics. However, the mechanism by which they lead to a reduction in the level of Akt phosphorylation is not clear. Recent work with PC-3 cells showed that enhancing PIP_3 production reduced the effectiveness of perifosine in blocking membrane localization of Akt.[6]

In support of ALP reducing Akt activation by a direct interaction with Akt, a number of techniques have been used to monitor the binding of these and related molecules to the isolated PH domain.[7−11] They indeed show that ALPs can bind to the isolated PH domain. However, the location at which perifosine and other ALPs bind to the PH domain in relation to the cationic cleft that binds PIP_3 is not known. An alternate mechanism for ALP cytotoxicity recently proposed involves indirect effects of the ALP on Akt1 activation. ALPs partition into membranes at low concentrations and interact strongly with cholesterol.[12,13] In doing so, they may disrupt the lipid raft domains needed for signaling.[14]

We have used the newly improved method of high-resolution field-cycling ^{31}P nuclear magnetic resonance (NMR) spectroscopy[15] to examine the binding of phosphoinositides and ALPs to the recombinant Akt PH domain. This technique, rooted in NMR relaxation theory, explores the physical properties of ^{31}P NMR absorption of phosphorylated amphiphiles in response to protein binding.[16,17] Changes in the rate of recovery (R_1) of the phosphorus nuclear spins are studied as a function of magnetic field, in a single automated attachment to a standard NMR spectrometer. The changes in R_1 can be dramatically enhanced by modifying cysteines on a protein of interest with unpaired electron spin-labels (such as nitroxides) near the anticipated binding site.[18,19] The unpaired electron of the spin-label will differentially relax phosphorus nuclear spins on ligands, depending strongly on how close the binding site is to the unpaired electron. The extracted paramagnetic relaxation

Received: December 30, 2013
Revised: January 1, 2014
Published: January 2, 2014

   dx.doi.org/10.1021/bi401720v | *Biochemistry* 2014, 53, 462−472

enhancement of R_1 (PR_1E) can be used to estimate the location of the ligand binding site. The field-cycling method we use is considerably more sensitive and quantitative than line-broadening methods at fixed fields, which have been used extensively in the past. The technique is particularly useful for identifying novel lipid binding sites on a protein.[19,20]

Another useful feature of field-cycling NMR, utilized here for the first time, is its ability to detect the aggregation of the dominant species that is involved in low-field relaxation, from the shape of the low-field relaxation dispersion.

Using this method, we have monitored the binding of miltefosine and perifosine, as well as a soluble inositol derivative, to the recombinant Akt1 PH domain. We find that miltefosine and perifosine each bind to the PH domain but at sites spatially distinct from, although near to, the PIP_3 binding site. One of the ALPs, miltefosine, can also bind in the same region occupied by PIP_3. However, it is easily displaced by the more tightly binding PIP_3 molecule. The alternate amphiphile site is not occupied by PIP_3 or the soluble molecule inositol hexakisphosphate (IP_6). We argue that the primary mechanism whereby ALPs exert cytotoxic effects may not be by binding to the Akt PH domain PIP_3 site, but by binding in this new adjacent site and, in so doing, altering the orientation of the Akt1 protein on an interface so that it is no longer aligned for optimal binding to membranes and hence not aligned for phosphorylation. The existence of a novel site for amphiphiles on the Akt1 PH domain could provide a new target to exploit in regulating the intact Akt1 protein.

EXPERIMENTAL PROCEDURES

Chemicals. Dioctanoylphosphatidylinositol 3,4,5-trisphosphate (diC_8PIP_3) was purchased from Cayman Chemical. Perifosine was purchased from Selleck (Houston, TX). The spin-labeling reagent (1-oxyl-2,2,5,5-tetramethyl-Δ^3-pyrroline-3-methyl) methanethiosulfonate (MTSL) was purchased from Toronto Research Chemicals. Other chemicals used were obtained from Sigma-Aldrich.

Cloning, Overexpression, and Purification of Akt1 His_6-PH and Mutated Proteins. Human Akt1 cDNA was obtained from Origene. Polymerase chain reaction (PCR) primers (Integrated DNA Technologies) were designed to introduce restriction sites into the beginning (*Nde*I) and end, including a stop codon (*Sal*I-HF), of the PCR product. This results in a PCR product that encodes residues 1−131 (the PH domain) of Akt1. The PCR product, purified using the Qiagen PCR Purification Kit, and the pET28a vector (Novagen) were doubly digested with *Sal*I-HF and *Nde*I-HF (New England Biolabs) at 37 °C for 1 h. Ligation of the PCR product into the pET28a vector (EMD Biosciences) resulted in a gene that encodes the Akt1 PH domain with an N-terminal His_6 tag that aids in purification of the recombinant protein. The genes for the PH domain mutants W22C and T21C were constructed by site-specific mutagenesis using a mutagenesis kit from Stratagene. All mutations were confirmed by DNA sequencing (Genewiz). BL-21 STAR cells (a gift from E. Kantrowitz, Boston College), transformed with the plasmid containing the gene for His_6-PH, were grown overnight in LB medium (Fisher Scientific) supplemented with 30 μg/mL kanamycin. Aliquots of this suspension were added to LB medium supplemented with 30 μg/mL kanamycin sulfate, and the cultures were grown at 37 °C to an OD_{600} of 0.6−0.8. PH domain overexpression was induced with the addition of 0.1 mM IPTG followed by incubation either at 24 °C for 4 h or at 16 °C overnight. After centrifugation of the suspension, the cell pellet was stored at −20 °C until it was needed.

For protein purification (both wild type and the two cysteine mutants, W22C and T21C), cells were thawed and resuspended in ice-cold lysis buffer (PBS with 1% Triton X-100, 10 μg/mL leupeptin, 0.2 mM AEBSF, and 1 μM aprotinin). Lysozyme (1 mg/mL) was added to the lysate and the solution incubated while being shaken for 30 min at room temperature. DNase I and $MgCl_2$ were then added to final working concentrations of 40 units/mL and 10 mM, respectively, and the mixture incubated for 15 min while being shaken at room temperature. The lysates were centrifuged at 14000 rpm and 4 °C for 20 min, and the solution was further clarified by being passed through a syringe fitted with a 0.45 μm filter. Imidazole was added to a final concentration of 20 mM. The recombinant PH domain was purified from the crude protein fraction using an Ni-NTA resin (Qiagen). After the resin had been extensively washed, the PH domain was eluted with 100 mM imidazole in PBS. Fractions containing protein were first dialyzed at room temperature against 25 mM HEPES (pH 7.4), 75 mM NaCl, and 1 mM EDTA, followed by dialysis at 4 °C against the buffer with the NaCl concentration reduced to 20 mM. The dialyzed eluant was applied to a QFF column containing QFF washed with 25 mM HEPES and 1 mM EDTA (pH 7.4). The PH domain was eluted using a salt gradient from 0 to 600 mM NaCl in 25 mM HEPES (pH 7.4) and 1 mM EDTA. Fractions containing the recombinant protein were concentrated at 4 °C using a 10 kDa cutoff centrifugal concentrator and buffer exchanged into 25 mM HEPES, 125 mM NaCl, and 1 mM EDTA (pH 7.4). The CD spectrum of the recombinant PH domain proteins indicated that they are well-folded with significant β-sheet content. The protein concentration was checked by A_{280} using the extinction coefficient calculated with ProtParam.[21]

Spin-Labeling of the PH Domain. The concentrated His_6-PH in 20 mM HEPES and 125 mM NaCl (pH 7.4) was incubated with an excess of DTT for 45 min at room temperature and then applied to a spin column equilibrated with the same buffer to remove excess DTT. An aliquot of a 20 mg/mL acetone stock solution of MTSL was diluted in the protein buffer and added to the protein solution to generate a 10-fold molar excess of MSTL compared to total cysteine residues. After incubation for 3 h, excess spin-label was removed when the sample was passed through a spin column. Previous work has suggested that Cys77 is more reactive than Cys60 and could be the primary site of spin-labeling.[22] However, >80% of available cysteine residues in the recombinant PH domain and 89% of the cysteines in T21C were modified by MTSL as assayed by the reactivity of the spin-labeled denatured proteins with Ellman's reagent.

For NMR samples, the spin-labeled PH domain was diluted to 37 μM (unless otherwise indicated) in 20 mM HEPES, 125 mM NaCl, and 1 mM EDTA (pH 7.4) (with 50% D_2O), with various phosphorus-containing ligands added at concentrations of 2−5 mM.

High-Resolution ^{31}P Field-Cycling NMR Measurement. Each sample with a volume of of 260 μL was pipetted into a newly designed NMR sample system that is easily loaded and removed and can be used more conveniently for titrations (for details, see http://www.bio.brandeis.edu/faculty/redfield.html). The ^{31}P field-cycling spin−lattice relaxation rate (R_1) measurements were taken at 20 °C on a Varian Unity^{plus} 500 spectrometer using either a 5 or 10 mm Varian probe with a

custom-built device that can move the sample, from the usual sample probe to a higher position within, or just above, the magnet, where the magnetic field is between 0.04 and 10 T. Details of the spin−lattice relaxation rate ($R_1 = 1/T_1$) measurement at each field strength and data analysis have been described in detail previously.[16,19] Chemical shifts for multiply phosphorylated diC_8PIP_3 and IP_6 resonances have been assigned previously.[23,24]

NMR Data Analysis. ΔR_1, the relaxation due to the spin-label at each field (the paramagnetic R_1 relaxation enhancement or PR_1E), is obtained by subtracting the R_1 value obtained in the presence of protein without the spin-labels from R_1 for the same amphiphile in the presence of the spin-labeled protein. For a single spin-label on the protein, the expected field dependence of ΔR_1 can be characterized by only three parameters: (i) a scaling factor, $\Delta R_{P\text{-}e}(0)$, for the effect of the spin-label(s) on ^{31}P, (ii) a correlation time, $\tau_{P\text{-}e}$, which is usually the tumbling time of the protein−ligand complex, and (iii) a small baseline term, c, from smaller internal motion.[19] The PR_1E at each magnetic field is fit with the equation $\Delta R_1 = R_{P\text{-}e}(0)/(1 + \omega^2\tau_{P\text{-}e}^2) + c$. The parameters $R_{P\text{-}e}(0)$ and $\tau_{P\text{-}e}$ along with the spin-labeled PH domain total molarity, [PH], and the ligand molarity, $[L_o]$, are used to calculate a distance by

$$r_{P-e}^6 = ([PH]/[L_o])[\tau_{P\text{-}e}/R_{P\text{-}e}(0)][0.3\mu_o^2(h/2\pi)^2\gamma_P^2\gamma_e^2]$$

Here the constants in the product $\mu_o^2(h/2\pi)^2\gamma_P^2\gamma_e^2$ are defined in many texts on NMR.[25] The sixth root of this expression, $r_{P\text{-}e}$, is our estimated average distance between the ^{31}P and the nitroxide(s) when the ligand is bound, at least for diester phosphates. Because the PH domain has two spin-labels, $r_{P\text{-}e}$ is not a true distance but an average of the effects of both labels, except in cases where the effect of a single spin-label can be isolated (see below). Constants and assumptions in deriving this distance have been described in detail previously.[16,17,19] We omit the usual "order parameter" used in standard NMR theory because the distances with which we are dealing are relatively large.

The distances for the inositol ring monophosphates are also tabulated and might also provide approximate distances to spin-labels. However, we found for PIP_3 (Figure 2) that the relaxation behavior of all three monophosphates is nearly the same. From this, we might conclude that the inositol ring is oriented relative to the spin-label in a manner that makes these three ^{31}P nuclei at the same distance from the spin-label. We think that this would be highly unlikely, and we postulate that this behavior is most likely to be due to "spin diffusion", as it is called by the NMR community. Spin diffusion denotes the rapid exchange between nearby spins of the same type (in this case both ^{31}P) of spin energy by a process in which the dipolar interaction makes a pair of nearby spins, *a* and *b*, each concertedly flip to the opposite orientations, from *a* up and *b* down to *a* down and *b* up. Because of the slow tumbling of the aggregate, it is likely that this process would occur considerably more rapidly than the rate of relaxation of any of the three ^{31}P spins by the spin-label, and that the three adjacent monoesters would act as a single minipool each having the same apparent relaxation behavior for all three.

We also assume that the K_d values of all sites are low enough that all sites are saturated with 3−5 mM ligand, with the possible exception of the compound IP_6.

Modeling Binding of the Amphiphile to the PH Domain. Modeling was conducted in several stages. The protein models were retrieved from the Protein Data Bank (PDB) (entries 1UNP and 1UNQ, with IP_4 bound[3]) and visualized with COOT[26] and PYMOL.[27] The three-dimensional models for ligands (perifosine and miltefosine) were obtained using the web service PRODRG.[28] Energy-minimized structures were used for flexible ligand docking using the SWISSDock web service.[29] The PDB structures stripped of ligands and the solvent elements were used, and the ligands were docked to them. The 50 highest-scoring poses were retained and analyzed. Individual clusters were visualized (in COOT and PYMOL) and compared with the distances obtained in field-cycling NMR experiments. The highest-scoring poses were retained from the clusters that fulfilled the experimental distance constraints. Long acyl chains usually were bound in a somewhat disordered manner meandering on the protein surface. We deemed the amphiphiles were reliably docked when there was a match achieved between the ligand headgroup and the protein electrostatic signature. The remaining carbon atoms of the acyl chains were repositioned using the torsion angles to match the predicted approach direction to the membrane.

The uncertainty in the location of individual spin-labels was taken into account by establishing a sphere close to the covalently modified Cys residues, and the distances from the centers of these spheres to the docked phosphate groups of the ligands were measured. Usually, the highest-scoring poses of the binding compounds matched the distance constraints automatically when the correct cluster was considered. The results were visualized in PYMOL and the mutual relationships between docked compounds analyzed.

RESULTS

Field-Cycling Methodology: What Is Measured. High-resolution field-cycling ^{31}P NMR has been used previously by us to probe where phospholipids, presented in vesicles, bind to peripheral membrane proteins[19,20] as well as to quantify weak binding of small soluble molecules[18] to proteins. However, in this work, where we explore the site of binding of different amphiphiles, including the natural ligand PIP_3 as well as cytotoxic alkylphospholipids, to the Akt1 PH domain, short-chain phospholipids that form micelles in solution are used instead of vesicles. This is reasonable because the interaction of the PH domain with PIP_3 is headgroup-specific.[8] The narrower resonances of the micelles allow better resolution of ^{31}P resonances in mixtures of phospholipids. Because this is a relatively unfamiliar methodology, we summarize it below before giving the detailed results.

We directly observe the NMR signal of the 100% abundant nuclear spin of ^{31}P of diverse phospholipids, in the presence of a lower molarity of the PH domain, here 0.004−0.012 molar ratio of protein to the ^{31}P-containing ligand. The PH domain naturally contains two cysteine residues on its surface, at positions 60 and 77; in later experiments, a third spin-label is added at one of two other positions, in the constructs T21C and W22C. The spin-label chemically attached to each cysteine contains an unpaired electron spin that has a magnetic moment ~700 times that of the protons surrounding the ^{31}P. Spin-labels act here as simple magnets of well-understood properties that provide a very well localized magnetic field, because of their electron spin, that noticeably affects the ^{31}P nuclear spins more than 2 nm away.

The spin−lattice relaxation rate R_1 of the one or more ^{31}P spins on the lipid is much larger when the ^{31}P-containing lipid

dx.doi.org/10.1021/bi401720v | *Biochemistry* 2014, 53, 462−472

is bound near the spin-label on the PH domain than when the lipid is free in solution. The free-in-solution species is detected after a delay time, t_d, at a low magnetic field. The NMR sequence utilizes field cycling in such a way that the observed signal always approaches zero for an infinite delay,[15] and we find that the amplitude of the subsequent signal can always be fit to a constant times $\exp(-R_1 t_d)$. The observed rate, R_1, is matched to be within the time scale of our measurement device, on the order of 100 ms or more, by choice of the molar ratio of the spin-labeled PH domain to phospholipid in the NMR tube.

The on-protein R_1 rate is frequency-dependent, and at very low fields, it is constant. At higher field runs, the rate decreases until the ^{31}P resonance frequency approaches the "half-point" field, $H_{1/2}$, defined as the field where the R_1 rate has decreased to half its low-field value. Above this field, the rate decreases further until it is obscured by another relatively uninteresting mechanism (chemical shift anisotropy), at high field. This behavior is seen in all the data where R_1 is plotted as a function of magnetic field, both for the micellar lipids by themselves[31] and with the spin-labeled protein.

Rather than tabulate this half-point field, $H_{1/2}$, for various lipids and spin-labeled PH domains in our tables, we convert it to a time τ defined as $\tau = 1/(\gamma_p H_{1/2})$, where $\gamma_p H_{1/2}$ is 2π times the ^{31}P NMR frequency at the half-point field, $H_{1/2}$. The time τ, or low-field correlation time, is of potentially great interest analytically, because 2τ is an estimate of the average time taken for rotational diffusion,[32] of the Akt PH domain complexed to an unknown number of lipids. The size estimate would be exact if the aggregate were spherical, but in any case, knowledge of the value of 2τ allows a crude estimate of the size of the aggregate. This knowledge is useful technically, because the short side-chain lipids used as surrogates for long-chain lipids form micelles whose sizes and CMCs could be affected by the presence of the PH domain.

Of greater relevance here is our ability to estimate the distance $r_{P\text{-}ee}$ from a spin-label on the Akt PH domain to the ^{31}P nuclear spin on the phospholipid, while the latter is bound to it for at least the length of the correlation time. The likely error in our distance measurements would be much better than 5% if the ^{31}P and spin-label were rigidly localized relative to each other or exhibited fast local motion that was spherical in deviation from a fixed location. Although the attached spin-label is flexible, the error in the average absolute distance should certainly be <2 Å. Comparing ^{31}P−spin-label distances derived for different ligands binding to the same spin-labeled protein should be more accurate because the nitroxide moiety should have the same mobility.

For the recombinant Akt1 PH domain, the spin-labels attached to Cys60 and Cys77 are indicated in Figure 1. In the crystal structure, the sulfhydryl groups of these cysteines are 6.7 Å from one another and between 9.8−16.4 Å (Cys77) and 15.9−22.1 Å (Cys60) from the phosphate groups of inositol 1,3,4,5-tetraphosphate. To isolate the relaxation due to the spin-label when the ^{31}P molecule is bound, ΔR_1, we obtain a field dependence of R_1 for the lipid in the presence of protein without the spin-labels and subtract it from the relaxation profile for the same amphiphile using spin-labeled protein. This enhancement of the relaxation rate (ΔR_1) measures the specific contribution of the spin-label(s) to ^{31}P relaxation (the PR_1E or paramagnetic R_1 relaxation enhancement) as a function of magnetic field.

The two useful parameters that are extracted from the variation of ΔR_1 with magnetic field at low fields are $\tau_{P\text{-}e}$ and

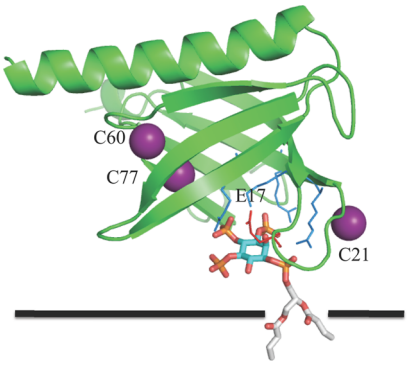

Figure 1. Crystal structure (PDB entry 1UNQ) of the Akt1 PH domain with IP_4 (to which a dibutyroylglycerol moiety is attached) bound. Amino acids in the cationic binding pocket that make contact with the IP_4 phosphate groups (orange and red) are colored blue. Cys60, Cys77, and T21C spin-labels are shown as magenta spheres. The oncogenic mutation site at Glu17 is colored red, and the postulated orientation of the membrane is depicted by the black plane.

$R_{P\text{-}e}(0)$, the magnitude of R_1 extrapolated to zero field. If only a single electron spin is dominant, the average distance of the bound nucleus to the spin-label is proportional to the sixth root of the $\tau_{P\text{-}e}/R_{P\text{-}e}(0)$ ratio. What the r^{-6} dependence means is that a 10% change in the distance between the ^{31}P and unpaired electron would lead to a 2-fold change in $R_{P\text{-}e}(0)$. Subtle changes in ligand binding can potentially be detected with this methodology. Larger changes in $R_{P\text{-}e}(0)$ can also be used to suggest discrete and spatially distinct binding sites for ligands. For accurately assessing longer distances, more protein is used. If more than one spin-label is present, the distance extracted, $r_{P\text{-}e}$, is an average that includes contributions from both labels. For spin-labels on (A) Cys60 and (B) Cys77, the extracted $r_{P\text{-}e}{}^{-6} = r_A{}^{-6} + r_B{}^{-6}$. As long as r_A exceeds r_B by more than 20%, the effect of site B can be ignored.

Interactions of the Akt1 PH Domain with a Phosphoinositide and IP_6. Initial experiments monitored the field-cycling profiles for diC_8PIP_3, a short-chain version of the natural PIP_3 ligand of the PH domain, as well as for the soluble ligand IP_6, which has been shown to bind to the PH domain.[8] The short octanoyl chains of diC_8PIP_3 cause this ligand to form small micelles at the millimolar concentrations that are desirable for field-cycling NMR. Dioctanoylphosphatidylinositol micelles are small in the absence of protein,[31] and adding three phosphate groups to the inositol ring is unlikely to make them significantly larger, at least in the absence of protein. The small micelle size for diC_8PIP_3 is indicated by only a very small increase in R_1 for non-spin-labeled protein compared to no protein at all. The change was only 0.1 s^{-1} after a minimum of ∼2 T had been reached.

Figure 2 shows the extra low-field dependence profile for diC_8PIP_3 in presence of the spin-labeled PH domain (37 μM). The gray line indicates the behavior of R_1 for these resonances in the presence of the same amount of unlabeled protein. A clear increase in the spin−lattice relaxation rate (R_1) at low field due to binding to the spin-labeled PH domain is observed for the phosphodiester resonance (P-1), and to a considerably lesser extent for the three phosphomonoesters. The vertical arrows in Figure 2 provide a visual estimate of the parameter $R_{P\text{-}e}(0)$, the relaxation rate extrapolated to zero field, for each of the resonances. However, the $\tau_{P\text{-}e}$ value extrapolated when bound to the PH domain is fairly large, 130 ns, suggesting that

dx.doi.org/10.1021/bi401720v | Biochemistry 2014, 53, 462−472

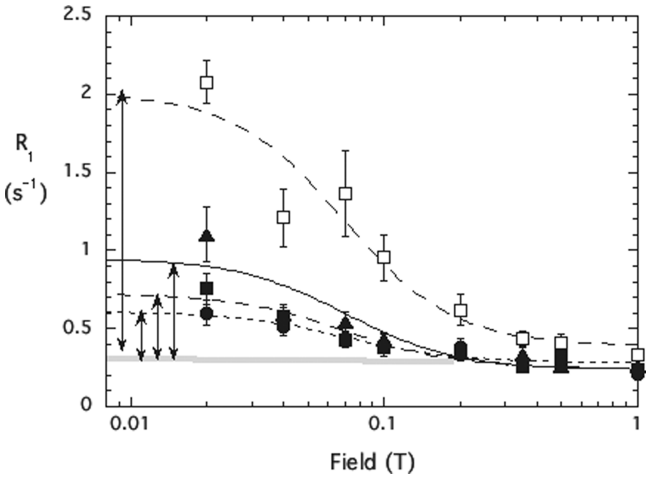

Figure 2. Variation of R_1, the spin−lattice relaxation rate, with magnetic field for ^{31}P resonances in diC$_8$PIP$_3$. The different ^{31}P atoms in the molecule are (□) phosphodiester, (▲) P(3), (■) P(4), and (●) P(5). The sample consisted of 3 mM diC$_8$PIP$_3$ with 37 μM Akt1 PH spin-label in 20 mM Hepes (pH 7.4), 125 mM NaCl, and 1 mM EDTA with 30% D_2O. The arrows estimate $R_{P\text{-}e}(0)$ for each of the different peaks; the gray line represents the limiting R_1 at low field for the phosphomonoesters with the unlabeled PH domain added.

the PH domain forms large micelles with the diC$_8$PIP$_3$ molecules. Relevant field-cycling parameters and $r_{P\text{-}e}^6$ values for each of the phosphorus resonances are listed in Table 1. If

Table 1. Parameters Extracted from High-Resolution Field-Cycling ^{31}P NMR Data for diC$_8$PIP$_3$ and IP$_6$ Binding to the Spin-Labeled Akt1 PH Domain (37 μM)

ligand[a]	$\tau_{P\text{-}e}$ (ns)	$\Delta R_{P\text{-}e}(0)$ (s^{-1})	r_{app}^6 ($\times 10^{84}$ m^6)	r_{app} (Å)
diC$_8$PIP$_3$				
P(1)	134 ± 41	1.62 ± 0.26	12.4	15.2 ± 0.8
P(3)	130[b]	0.71 ± 0.13	27.4	17.4 ± 0.9
P(4)	130[b]	0.48 ± 0.05	40.4	18.5 ± 1.0
P(5)	130 ± 49	0.32 ± 0.06	60.7	19.8 ± 1.3
IP$_6$ with EDTA				
P-1/P-3	217 ± 52	0.21 ± 0.02	92.6	21.3 ± 0.9
P-2	133 ± 60	0.23 ± 0.04	51.8	19.3 ± 1.5
P-4/P-6	206 ± 45	0.17 ± 0.01	109	21.8 ± 0.8
P-5	314 ± 156	0.24 ± 0.06	118	22.2 ± 2.0
IP$_6$ with Mg^{2+}				
P(2)	318 ± 153	0.21 ± 0.04	136	22.7 ± 1.9
P(4,5,6)	108 ± 35	0.18 ± 0.02	53.8	19.4 ± 1.1
P(1,3)	204 ± 81	0.24 ± 0.04	76.2	20.6 ± 1.4

[a]Ligand concentrations of 3 mM PIP$_3$ and 5 mM IP$_6$. [b]The data for P(3) and P(4) were fit to the average τ_{Pe} from the better defined profiles for P(5) and the phosphodiester, P-1.

the PH domain binds to only a single diC$_8$PIP$_3$ molecule, the correlation time would be smaller, certainly <20 ns. For a protein−diC$_8$PIP$_3$ micelle complex in which one of the molecules is bound moderately tightly to the protein, the correlation time should reflect overall micelle tumbling and be considerably longer. The value of 130 ns would be consistent with the formation of such a large complex.

The value of $r_{P\text{-}e}^6$ (and $r_{P\text{-}e}$) for the phosphodiester linkage (P-1) is considerably smaller than for any of the phosphate groups on the inositol ring (P-3, P-4, and P-5), as seen from the much smaller increase in the observed R_1 for the latter resonances. While this undoubtedly signals differences in the distance of the ^{31}P nuclei in the inositol ring from the spin-labels, the conclusion for the inisitol ring monophosphates is obscured by spin-diffusion as described in Experimental Procedures. Because nearly all the other ligands examined are phosphodiesters, that diC$_8$PIP$_3$ resonance will be used for comparison to the alkylphospholipids.

If we assume that the bulk of the relaxation is from only one of the two nitroxides on the protein (Cys77 is closer to the PIP$_3$ site than Cys60), the average $r_{P\text{-}e}$ value for P-1 is 15.0 ± 0.8 Å. The distance obtained is reasonable given the location of Cys77 compared to the PIP$_3$ binding site identified in the crystal structure. The other distances for P-3, P-4, and P-5 indicate qualitatively that the ring is farther from one or both of the spin-labels in the bound orientation.

IP$_6$ has been thought to bind weakly to the cationic binding site of the PH domain.[8] The field dependence of R_1 for 5 mM IP$_6$ bound to the same concentration of the spin-labeled PH domain (Figure 3) does indeed show an increase in R_1 in all of

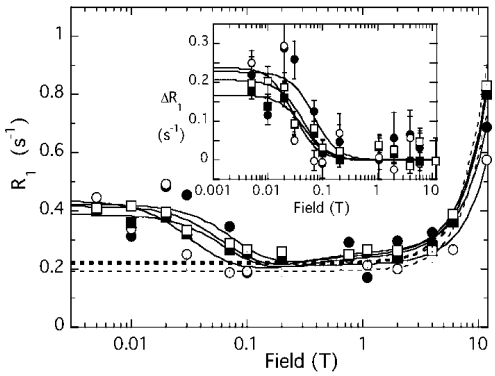

Figure 3. Field dependence of ^{31}P R_1 for the four resonances of IP$_6$ (5 mM) in the presence of 37 μM Akt-PH-SL: (□) P(1/3), (●) P(2), (■) P(4/6), and (○) P(5). The inset shows the change in R_1 due to the spin-labels as a function of field comparing the sample subtesla rates to those obtained with the unlabeled Akt1 PH domain (···).

the phosphate resonances, although these values are 2−3-fold smaller than what is seen for the diC$_8$PIP$_3$ phosphomonoesters. The average correlation time for the IP$_6$−PH domain complex, 220 ± 70 ns, is much longer than would be expected for a soluble small molecule binding to a protein the size of the PH domain, and somewhat larger than what is observed with diC$_8$PIP$_3$ binding. This indicates that IP$_6$ binding causes aggregation of the PH domain, probably to a somewhat greater degree than does diC$_8$PIP$_3$ binding.

Because Mg^{2+} is often included in the buffers for binding experiments with the PH domain, the field cycling was repeated with that divalent cation present. Mg^{2+} alters the IP$_6$ chemical shifts and causes overlap of two of the four resonances (data not shown), which combined with larger line widths made them difficult to definitively identify. Despite these changes, $R_{P\text{-}e}(0)$ values are similar with and without Mg^{2+}, and $\tau_{P\text{-}e}$ values are similar despite the significant errors (Table 1). The average $r_{P\text{-}e}^6$ value is the same within error with or without Mg^{2+} and marginally within the error for the average of the phosphomonoesters of diC$_8$PIP$_3$.

Binding of Cytotoxic Alkylphospholipids to the Akt1 PH Domain. It has been proposed that the cytotoxicity of the alkylphospholipids miltefosine (hexadecylphosphocholine) and

dx.doi.org/10.1021/bi401720v | Biochemistry 2014, 53, 462−472

perifosine [octadecyl(1,1-dimethyl-4-piperidylio) phosphate] occurs via inhibition of Akt activation, presumably by their binding to the PH domain and preventing membrane translocation of Akt.[4] To determine whether this was a plausible mechanism, field cycling was used to explore whether these drugs are capable of binding to the PH domain and if they occupy the same binding site as the natural ligand diC_8PIP_3.

Miltefosine is a zwitterionic amphiphile that has a single alkyl chain and a phosphocholine polar group; the CMC for pure miltefosine has been reported to be 12.4 μM.[33] R_1 as a function of field for 5 mM miltefosine with the Akt1 PH domain (0.6 mg/mL or 37 μM unlabeled protein) added shows a small increase in relaxation rates at all fields compared to those for miltefosine alone (Figure 4). Analysis of the field dependence profile for miltefosine alone shows a 19 ± 5 ns correlation time that is basically the same, 20 ± 2 ns, as with the unlabeled protein added.

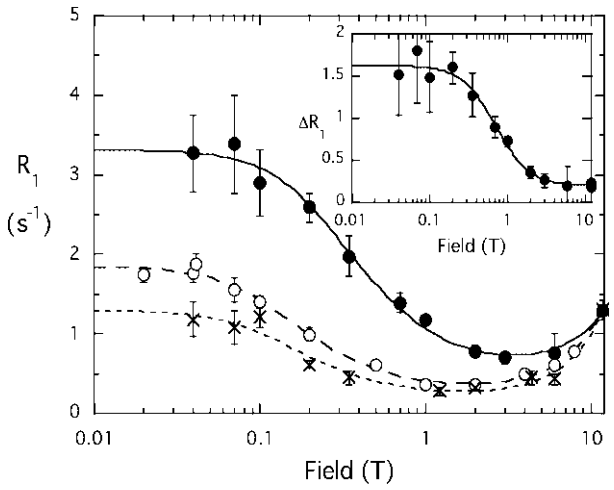

Figure 4. Effect of the spin-labeled Akt1 PH domain on the field dependence of miltefosine ^{31}P R_1. The miltefosine (5 mM) ^{31}P R_1 profile is shown in the absence of protein (×) and in the presence of the unlabeled (○) or spin-labeled (●) His_6-tagged Akt1 PH domain (37 μM). The inset shows the portion of ^{31}P R_1 due to the proximity to the spin-labels on the PH domain, ΔR_1.

When miltefosine is mixed with the spin-labeled Akt1 PH domain, there is a further increase in R_1 at low fields (Figure 4), indicating that the complex formed is sufficiently close to the spin-labels to be relaxed. From the field dependence of ΔR_1 (shown in Figure 4, inset), $r_{P\text{-}e}{}^6$ is 0.83 × 10^{-54} m^6, a value much smaller (~15-fold) than what was observed for the phosphodiester resonance of diC_8PIP_3. This translates to a miltefosine $r_{P\text{-}e}$ distance 5 Å closer to the spin-label than measurements indicated for PIP_3. This suggested that one or more miltefosine molecules must be binding in a site different from that of diC_8PIP_3, so that the miltefosine ^{31}P is closer to the spin-labels than the P-1 of diC_8PIP_3 is (Table 2). Significantly, $\tau_{P\text{-}e}$ remains nearly the same as the correlation time for micelles alone, indicating that there is no large difference in size between the miltefosine micelles and the PH domain−miltefosine complex.

The field dependence of miltefosine in the presence of both IP_6 and the spin-labeled PH domain was also obtained (data not shown). The extracted $\tau_{P\text{-}e}$ and $R_{P\text{-}e}(0)$ values for miltefosine were not changed by the addition of IP_6, suggesting that IP_6 does not compete for binding to the miltefosine site(s) relaxed by spin-labeled Cys77 (and Cys60). However, the field dependence profile for IP_6 was very much affected by the addition of miltefosine: the small but reproducible increase in IP_6 R_1 values at low fields caused by the spin-labeled PH domain was reduced with miltefosine present. The much smaller correlation time for the miltefosine−spin-labeled PH domain complex (Table 2) indicates that the aggregation induced by IP_6 binding does not occur with miltefosine present.

Perifosine is another zwitterionic alkylphospholipid that has been shown to be cytotoxic to tumor cells and is currently in clinical trials for several solid tumors and multiple myeloma, albeit with marginal results in current studies.[4] The alkyl chains in this compound are longer than in miltefosine or diC_8PIP_3, so they might be expected to form larger micelles. The spin-labeled protein produces a much larger increase in the ^{31}P R_1 for perifosine (Figure 5) than in that for miltefosine. The correlation time is also longer, consistent with a larger micelle size (Table 2). There also appear to be two distinct dispersions at high and low fields (Figure 5, inset) that can be fit with two correlation times, one in the tens of nanoseconds and the other in the 1−5 ns range.

Whether one uses the single-dispersion fit or instead the slower correlation time of the two-dispersion fit, $r_{P\text{-}e}{}^6$ is only twice as large (Table 2), as inferred from the longer correlation time part of the dispersion for perifosine compared to that for miltefosine. The cationic moieties esterified to the phosphate of perifosine and miltefosine are different, one a choline and the other a piperidine, and this could affect the orientation of the ^{31}P with respect to the spin-label when the molecule is bound. However, the phosphodiesters of both these amphiphiles have an $r_{P\text{-}e}$ of 10−11 Å, significantly smaller than the value of 15 Å of the diC_8PIP_3 phosphodiester phosphorus, again suggesting the possibility of a second binding site.

Table 2. Parameters Extracted from High-Resolution Field-Cycling ^{31}P NMR Data for the Effect of the Spin-Labeled Akt PH Domain (37 μM) on the Phosphodiester ^{31}P in Alkylphospholipids and $diC_8PI(3,4,5)P_3$

ligand[a]	$\tau_{P\text{-}e}$ (ns)	$R_{P\text{-}e}(0)$ (s^{-1})	$r_{app}{}^6$ (×10^{54} m^6)	r_{app} (Å)
miltefosine	13.1 ± 1.4	1.42 ± 0.06	0.83	9.7 ± 0.2
miltefosine with IP_6	12.4 ± 2.5	1.32 ± 0.12	0.84	9.7 ± 0.3
perifosine				
single τ	67 ± 25	4.26 ± 0.63	1.41	10.6 ± 0.7
two τ				
slow τ	75 ± 21	3.86 ± 0.45	1.74	11.0 ± 0.5
fast τ	1.9 ± 0.6	1.14 ± 0.45	0.15	7.3 ± 0.4
diC_8PIP_3 P-1	134 ± 41	1.62 ± 0.26	12.4	15.2 ± 0.8

[a]Ligand concentrations of 5 mM alkylphospholipid, 5 mM IP_6, and 3 mM diC_8PIP_3.

dx.doi.org/10.1021/bi401720v | Biochemistry 2014, 53, 462−472

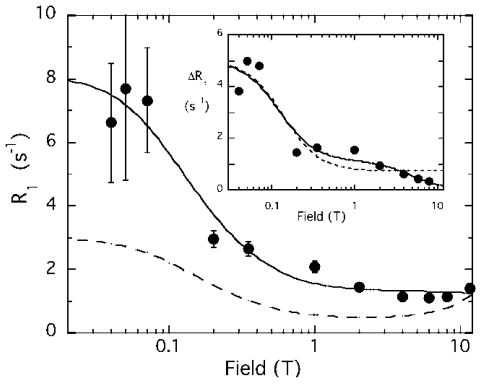

Figure 5. Field dependence of the perifosine (5 mM) ^{31}P in the presence of 37 μM Akt1 His$_6$-PH-SL (●) compared to the control where the protein is not spin-labeled (---). The inset shows the fits to the increase in R_1 due to the spin-labeled protein using a single correlation time, 67 ns (···), or two correlation times (—) for the ^{31}P–e complex and a high-field constant CSA of 75 and 1.9 ns.

When the parameter $r_{P\text{-}e}^6$ is calculated from the fast perifosine–spin-label correlation time, the value is quite small, indicating that on this faster time scale several perifosine molecules interact with the protein and are relaxed by the spin-labels.

These field-cycling experiments show that ALP molecules bind to the PH domain with at least one bound molecule having a longer residence time at a discrete site in a location different from the cationic site occupied by diC$_8$PIP$_3$ (which also forms micelles at the concentrations used). The ALPs might still occupy the PIP$_3$ site, but there is a separate binding site for them that is very effectively relaxed by the spin-label on Cys77 (and possibly by Cys60).

Binding of Alkylphospholipids to the Cationic Cleft of the Akt1 PH Domain Probed with a Third Spin-Label. The two naturally occurring Cys residues in the Akt1 PH domain are relatively far from the PIP$_3$ binding cleft. To see whether alkylphospholipids compete with PIP$_3$ binding in the cationic site, we engineered a third Cys into the PH domain by generating W22C and T21C variants. As predicted, a spin-label at either of these sites dramatically relaxed the diC$_8$PIP$_3$ phosphodiester resonance much more than the original spin-labeled PH domain (Figure 6A). Because the correlation times are approximately the same, 130 ns, for this ligand binding to the different spin-labeled PH domains (wild type with spin-labeled Cys60 and Cys77 compared to the W22C or T21C mutant with three spin-labels attached), we can subtract $R_{P\text{-}e}(0)$ for the original spin-labeled protein from the value for the new construct with three spin-labels and use this extra relaxation rate to determine a distance specifically from the spin-label on either of the new spin-labels on the Cys residues introduced at position 21 or 22. The value of $r_{P\text{-}e}$ for the distance from P-1 to W22C (from data for P-1 shown in Figure 8A) is ~9.5 Å. DiC$_8$PIP$_3$ was also examined with a lower concentration of spin-labeled T21C (data not shown). The extrapolated distance between the P-1 and the introduced spin-label ($r_{P\text{-}e}$) was 10.8 Å.

When 5 mM miltefosine is measured with spin-labeled Akt1 PH domain W22C, the relaxation profile is also significantly enhanced (compare Figure 6A to Figure 4A). The large increase in the level of relaxation for miltefosine indicates bound miltefosine must also be near (and very likely in) the PIP$_3$ site. The $r_{P\text{-}e}^6$ for miltefosine with spin-labeled W22C is 0.39×10^{-54} m^6. When both diC$_8$PIP$_3$ (3 mM) and miltefosine

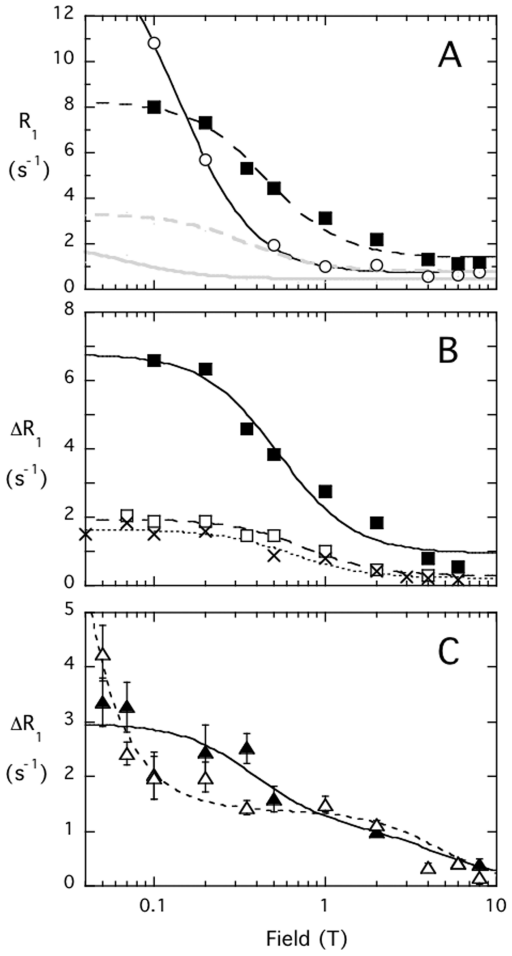

Figure 6. Effect of spin-labeled W22C or T21C of the Akt1 PH domain on the field dependence of ^{31}P R_1 of different amphiphiles. (A) R_1 profiles for 3 mM diC$_8$PIP$_3$ (○) or 5 mM miltefosine (■) with 37 μM spin-labeled W22C; the effects of the spin-labeled wild-type PH domain on diC$_8$PIP$_3$ (solid gray line) and miltefosine (dashed gray line) are also shown. (B) The R_1 component for miltefosine due to the spin-labeled W22C in the absence (■) or presence (□) of 3 mM diC$_8$PIP$_3$ is shown. For comparison, the effect of the PH domain (37 μM) with spin-labels only at Cys60 and Cys77 is shown (×). (C) ΔR_1 for binding of 5 mM perifosine to 19 μM spin-labeled Akt1 PH domain T21C in the absence (▲) or presence (△) of 0.1 mM diC$_8$PIP$_3$. The curves are fit to show two distinct dispersions, the faster fixed at a $\tau_{P\text{-}e}$ of 2 ns.

(5 mM) are present with the protein, the relaxation enhancement for the miltefosine phosphodiester is significantly reduced (the lower concentration for the diC$_8$PIP$_3$ P-1 peak and its fast relaxation along with its close chemical shift to the larger miltefosine meant its field dependence could not be accurately monitored). Figure 6B shows the change in miltefosine R_1 due to the additional spin-label on W22C as well as on Cys77 and Cys60. The profile for binding of miltefosine to labeled W22C with diC$_8$PIP$_3$ added is very similar to what was observed for miltefosine with the original spin-labeled (Cys60 and Cys77) PH domain, enhanced slightly because the spin-label on W22C should contribute some R_1 enhancement for the novel miltefosine site. This loss of much of the miltefosine PR_1E is attributed to PIP$_3$ displacing miltefosine from the phosphoinositide site. If we use $\Delta R_{P\text{-}e}(0)$, we estimate a distance of the miltefosine ^{31}P to the unpaired electron attached to W22C of 8.6 Å. Thus, miltefosine

dx.doi.org/10.1021/bi401720v | Biochemistry 2014, 53, 462–472

can bind in two discrete sites, one overlapping with the PIP_3 site that is easily displaced by diC_8PIP_3 and the other closer to the two original cysteines and not displaced by PIP_3.

Perifosine binding was also examined with a PH domain containing a spin-labeled cysteine near the PIP_3 site, in this case using mutant protein T21C (Figure 6C). Half as much protein was used in this experiment as well as a higher ALP concentration compared to what was obtained with spin-labeled wild-type protein, because if R_1 was enhanced to the same extent as with miltefosine we would not be able to easily monitor it given the larger correlation time for these micelles. Again, as seen with Figure 5, the ΔR_1 profile has two discrete dispersions, one with a 2 ns correlation time and another with a longer correlation time (~20−30 ns). The $r_{P\text{-}e}^6$ from the slower motion, 1.27×10^{-54} m^6, has been reduced to only 75% of the value for the spin-labeled wild-type protein, indicating only a small contribution to R_1 from the spin-label introduced on T21C. This suggests that perifosine does not fit well in the PIP_3 site. Another interesting part of the perifosine field dependence with T21C is that there is a comparatively larger ΔR_1 component for the faster dispersion (compared to what is seen with the spin-labeled wild-type protein). This is consistent with the more tightly bound perifosine(s) also bringing other ALPs together to form a micelle whose molecules interact loosely with the protein near the new spin-label site for up to a few nanoseconds. When 0.1 mM diC_8PIP_3 is added to the sample, there is a change in the field dependence profile at the lowest fields. The amount of PIP_3 added should occupy the canonical site on the PH domain. There is little effect on the perifosine dispersion associated with a 2 ns correlation time. However, the slower dispersion is shifted to lower fields consistent with the formation of a larger aggregate (longer $\tau_{P\text{-}e}$) and a perifosine molecule bound to the protein for that time (estimated to be between 100 and 200 ns). The smaller overall relaxation of perifosine by a spin-label on T21C and the smaller loss of PR_1E when PIP_3 is added to the protein are consistent with poor binding of that ALP in the PIP_3 site.

Modeling the Two Amphiphile Sites. The field-cycling experiments provide useful constraints for the three-dimensional model of the alkylphospholipids binding to the PH domain. The distances derived from the data are not absolutely accurate values for several reasons. For the spin-labeled wild-type PH domain, there is the unavoidable interference from two closely positioned spin-labels at positions 60 and 77. Perhaps, more importantly, amphiphilic ligand binding is likely to lead to a conformational change in the protein. In our modeling, we utilized the data obtained from the mutated protein when a third label was introduced at position 21 or 22. The distance estimates were more reliable because the influence of the double label (at positions 60 and 77) could be subtracted.

The $r_{P\text{-}e}$ distances obtained in this field-cycling experiment indicate that the diC_8PIP_3 is bound to the Akt1 PH domain in agreement with the crystallographically determined mode for IP_4. This orients the phosphodiester toward the 20s loop (Figure 1). The distances obtained for the perifosine and miltefosine indicate that the phosphodiesters of these amphiphilic molecules are closer to the 80s loop. These distance constraints combined with the analysis of the surface electrostatics of the protein indicated that the second binding site is most likely located near the original binding site for the inositol moiety of the PIP_3 but with the cationic part of the headgroup oriented toward Tyr18 and Glu17 (shown for perifosine in Figure 7A). The placement of both alkylphospholipids at this location conforms to the distance constraints

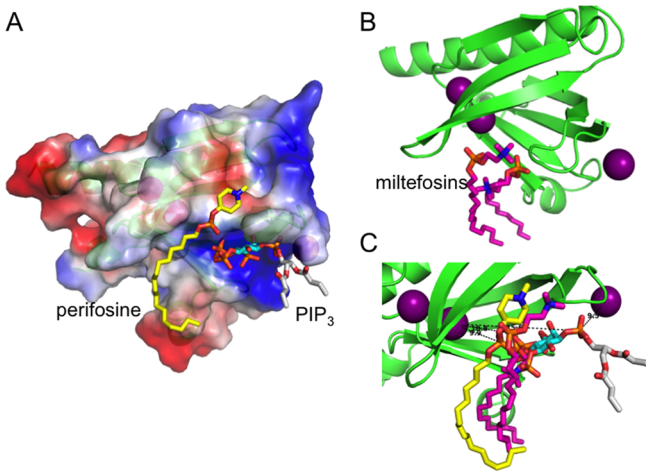

Figure 7. Modeling of diC_8PIP_3 and alkylphospholipids onto the PH domain of Akt1. (A) Surface representation of the PH domain of human Akt1 with the electrostatic potential mapped. Crystallographic IP_4 (with the diacylglycerol moiety of PIP_3 added) is shown in elemental colors, while perifosine carbon atoms are colored yellow. (B) Two miltefosine molecules are presented docked to the PH domain with one in the PIP_3 site and the other bound in a location similar to that of the perifosine molecule. (C) All the molecules with the distances between the diester phosphate groups and the fluorophores are marked. The distances agree remarkably well with the NMR results. In panel C, perifosine is colored yellow, $diC_8PIP(3,4,5)P_3$ is colored orange and cyan, miltefosine is colored magenta, and the spin-labels are the purple spheres. Two amphiphiles, either two miltefosine molecules or PIP_3 and either miltefosine or perifosine, can bind near one another in this region.

provided by NMR. The difference in the size of the headgroup between miltefosine and perfosine could explain the ability of both to bind at the novel second site while only the smaller miltefosine molecule binds to the PIP_3 site. The PIP_3 site has a well-defined electrostatic signature where individual phosphate groups are bound to the individual Arg residues filling in a relatively large protein pocket created by the twisting strands of the β-barrel of the PH domain (Figure 7).

The location of the main binding site as well as the site described in this work conforms to our understanding of how the PH domains interact with the membranes. The acyl chains are directed downward in Figure 1, which is the postulated direction of the membrane. All the phosphate groups are approximately bound at the same translational layer that delineates the boundary of the membrane. If the PH domain approaches from the electrostatically preferred direction, the binding of the individual phospholipids would require only marginal rearrangement of the membrane and only partial withdrawal of the hydrophobic acyl chains, thus binding Akt1 to the membrane. The existence of the second amphiphile site also provides an explanation for why the oncogenic Glu17 mutation is fairly resistant to ALPs (Figure 8). Glu17 appears to be critical for the Akt1 (as well as GRP1[34]) PH domain to bind PIP_3 with such selectivity.[8] Mutation of Glu17 significantly enhances the affinity of the domain for $PI(4,5)P_2$.[8,34] Given the higher concentrations of $PI(4,5)P_2$ in membranes, this should keep the protein membrane anchored. In our model, Glu17 also interacts with the cationic moieties of perifosine and

dx.doi.org/10.1021/bi401720v | Biochemistry 2014, 53, 462−472

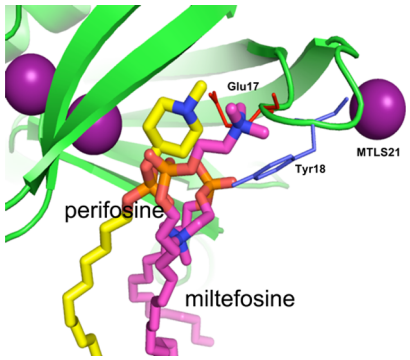

Figure 8. Model showing two miltefosine molecules (magenta) bound, one partially in the PIP_3 site and the other with the choline anchored by Glu17 and Tyr16, and a single perifosine (yellow) bound in the amphiphile site.

miltefosine and stabilizes their binding to the PH domain. When this interaction is not possible, the alkylphospholipids would be much less effective in altering membrane binding and hence phosphorylation of Akt1.

DISCUSSION

The protein kinase Akt is a critical enzyme in cell growth and proliferation.[1] Its tight binding of PIP_3 by the PH domain transiently anchors it to the plasma membrane for phosphorylation events that enhance its activity as a kinase. A number of drugs, including alkylphospholipids, reduce the level of Akt phosphorylation and alter the disposition of the protein on the membrane.[5,6] However, there is considerable debate over exactly what conformational change is induced by PIP_3 binding and whether the alkylphospholipids are cytotoxic because of binding to Akt and preventing membrane translocation or work by an alternative mechanism.[12,14,35,36] Binding studies in the literature show partitioning of the isolated PH domain to membranes as well as binding by ALPs, but they cannot tell where binding sites for ALPs are located.

High-resolution field-cycling ^{31}P NMR spectroscopy is an ideal method for characterizing the binding of the spin-labeled Akt1 PH domain to a short-chain version of its natural ligand, as well as to cytotoxic phospholipids that have been suggested to bind to this protein as part of their mechanism of toxicity. The recombinant Akt PH domain has two cysteine residues that are spatially close with one of them, Cys77, potentially more reactive to sulfhydryl reagents. Modification of the domain with methylglyoxal[22] labels only Cys77, and PIP_3 binding enhances this covalent modification. In intact Akt, the methylglyoxal-modified Akt is also activated.[22] The spin-labeled recombinant PH domain may also be in an activated state, and the ligand sites we detect may reflect approaching the activated conformation of the protein.

Our data for the spin-label on T21C are consistent with the PIP_3 headgroup oriented similarly to that seen in the crystal structures[2,3] of the Akt1 PH domain with the soluble headgroup analogue IP_4 bound (PDB entry 1UNQ). Our data also show that IP_6, which is also a ligand of the PH domain,[8] causes aggregation of this protein as evidenced by an uncharacteristically large ^{31}P electron correlation time for the spin-labeled PH domain complex with IP_6. A large aggregate is also seen when diC_8PIP_3 interacts with the PH domain; the correlation time for the ^{31}P–electron interaction is much larger than for any of the other micelle systems examined. The aggregation may be caused by charge neutralization of the highly anionic PIP_3 it is bound to the cationic region of the protein. It is possible that aggregation of the protein when very anionic ligands bind has a physiological role *in vivo*. For example, aggregation of Akt1 via binding of the PH domain to PIP_3 could cluster proteins for more efficient phosphorylation.

The two cytotoxic alkylphospholipids, miltefosine and perifosine, also bind to the isolated PH domain, but our data show that the binding occurs primarily at a site near, but distinct, from the PIP_3 site. One of the ALPs, miltefosine, can bind to the site occupied by PIP_3 but is very easily displaced by added diC_8PIP_3. The exclusion of miltefosine from the cationic cleft with diC_8PIP_3 present argues that alkylphospholipids likely function by doing something other than competing with PIP_3 for the cationic cleft. The second discrete ALP site is closer to Cys77 than is the phosphodiester of bound PIP_3 and does not directly overlap with the PIP_3 site.

Modeling predicts the location of the two possible binding sites for miltefosine: one overlapping with the PIP_3 binding site and the second on the side of the molecule in the proximity of the PIP_3 binding site (Figure 7B). Perifosine, with a larger headgroup, primarily binds at the new site and has a weaker affinity for the PIP_3 site. The placement of the phosphodiester bond in the crystallographic structures also agrees well with the expected distance to the new spin-label introduced at position 21 (~10 Å).

The previously suggested interaction of the PH domain with the membrane by the means of free interfacial loops (20s, 50s, and 80s) assumes that all the amphiphilic compounds provide a means of surface localization of the Akt1 protein. However, while the positioning of the inositol ring and the tight binding of the PIP_3 would position the entire kinase domain much more stringently at the membrane surface so that it can undergo the phosphorylation events necessary for activation, the single-chain miltefosine and perifosine molecules fit more loosely onto the protein. Additionally, because these molecules lie on the side of the PH domain, they would be expected to tilt the entire domain and skew the interfacial helix in such a manner that phosphorylation could be impaired.

Current views on what contributes to the cytotoxicity of alkylphospholipids toward cancer cells suggest that below their CMCs (typically in the low micromolar range), these lipids will insert into the plasma membranes of cells, while above the CMC, they would insert as small oligomers.[12] They are then translocated to the inner membrane by ATP-dependent lipid flippases or by lipid raft-dependent endocytosis.[5] Miltefosine has been shown to have an affinity for cholesterol,[12,36] and several alkylphospholipids have been shown to disrupt cholesterol homeostasis and hence alter lipid microdomains.[14] The reduction in the level of Akt membrane partitioning caused by these lipids could be overcome if more PIP_3 is produced by increasing the level of the PI3K catalytic subunit in cells; conversely, a myristoylated Akt, which partitions to the membrane without the aid of the PH domain, reduces the effectiveness of perifosine.[6] Both effects could be rationalized by effects of the alkylphospholipids on the raftlike domains that are likely the sites of Akt transient binding. This is an interesting alternative to the original thought that the alkylphospholipids bind to the Akt PH domain and prevent its membrane translocation.

However, our field-cycling work identifying two close but distinct amphiphile sites on the Akt1 PH domain modifies both views of ALP action. PIP_3 binds in only the well-recognized

phosphoinositide binding site, while the ALPs can access a nearby site that misorients the protein when it approaches the membrane. Alternatively, by binding in this second site, the latter could alter the affinity of the domain for PIP_3 or the residence time of the protein on the membrane. There may be a difference in the affinity of the ligands for the two sites, a difficult parameter to measure in a membrane. Although high-resolution field cycling is useful for quantifying weak binding ligands,[18] it lacks the sensitivity to measure micromolar affinities.

Our observation that binding of diC_8PIP_3 to the PH domain caused aggregation over and above the size of a simple protein−micelle complex also might suggest that this is what excess PIP_3 in a membrane could do with the PH domain even with cytotoxic amphiphiles present. The distinct site on the isolated Akt1 PH domain occupied by the ALPs is in the vicinity of a site on intact Akt1 that is occupied by various hydrophobic small molecules.[37] That site in Akt1 bridges both the catalytic and PH domains and maintains the kinase in a closed conformation. The site we have identified on the isolated PH domain is not the same, but it is possible that the ALPs could bind in that region in the intact protein, as well. Clearly, the new amphiphile site is novel and requires further investigation to determine a more detailed location on the PH domain and further refine what amphiphiles prefer to bind in that region and whether they populate intact Akt1.

High-resolution field-cycling NMR is beginning to be used in the area of protein dynamics[38,39] as well as with protein−membrane interactions. However, the PR_1E exploited here is particularly useful for defining interactions of an amphiphile with a protein. The methodology in this report shows that one need not have a single spin-labeled site on a protein to obtain information about discrete amphiphile sites on a protein. Whether the amphiphile is presented in a vesicle[19] or micelle (as in this study with the Akt1 PH domain), differences in the proximity of the amphiphile to spin-labels can be easily monitored. Combining the NMR $r_{P\text{-}e}$ distances with modeling can also provide insights into the position of the discrete amphiphile binding site.

AUTHOR INFORMATION

Corresponding Author

*E-mail: mary.roberts@bc.edu. Phone: (617) 552-3616. Fax: (617) 552-2705.

Funding

This work was supported by National Science Foundation Grant MCB-0517381 (M.F.R.).

Notes

The authors declare no competing financial interest.

ABBREVIATIONS

ALP, alkylphospholipid; CMC, critical micelle concentration; diC_8PIP_3, dioctanoylphosphatidylinositol 3,4,5-trisphosphate; DTT, dithiothreitol; IP_6, inositol hexakisphosphate; MTSL, (1-oxyl-2,2,5,5-tetramethyl-Δ^3-pyrroline-3-methyl) methanethiosulfonate; PH, Pleckstrin homology; PIP_2, phosphatidylinositol 4,5-bisphosphate; PIP_3, phosphatidylinositol 3,4,5-triphosphate; PR_1E, paramagnetic R_1 relaxation enhancement; R_1, spin−lattice relaxation rate.

REFERENCES

(1) Hers, I., Vincent, E. E., and Tavaré, J. M. (2011) Akt signalling in health and disease. *Cell. Signalling 23*, 1515−1527.

(2) Thomas, C. C., Deak, M., Alessi, D. R., and van Aalten, D. M. F. (2002) High-resolution structure of the pleckstrin homology domain of protein kinase B/Akt bound to phosphatidylinositol (3,4,5)-trisphosphate. *Curr. Biol. 12*, 1256−1262.

(3) Milburn, C. C., Deak, M., Kelly, S. M., Price, N. C., Alessi, D. R., and van Aalten, D. M. F. (2003) Binding of phosphatidylinositol 3,4,5-trisphosphate to the pleckstrin homology domain of protein kinase B induces a conformational change. *Biochem. J. 375*, 531−538.

(4) Gills, J. J., and Dennis, P. A. (2009) Perifosine: Update on a novel Akt inhibitor. *Curr. Oncol. Rep. 11*, 102−110.

(5) van Blitterswijk, W. J., and Verheij, M. (2013) Anticancer mechanisms and clinical application of alkylphospholipid. *Biochim. Biophys. Acta 1831*, 663−674.

(6) Kondapaka, S. B., Singh, S. S., Dasmahapatra, G. P., Sausville, E. A., and Roy, K. K. (2003) Perifosine, a novel alkylphospholipid, inhibits protein kinase B activation. *Mol. Cancer Ther. 2*, 1093−1103.

(7) Frech, M., Andjelkovic, M., Ingley, E., Reddy, K. K., Flack, J. K., and Hemmings, B. A. (1997) High affinity binding of inositol phosphates and phosphoinositides to the pleckstrin homology domain of RAC/protein kinase B and their influence on kinase activity. *J. Biol. Chem. 272*, 8474−8481.

(8) Landgraf, K. E., Pilling, C., and Falke, J. R. (2008) Molecular mechanism of an oncogenic mutation that alters membrane targeting: Glu17Lys modifies the PIP lipid specificity of the AKT1 PH domain. *Biochemistry 47*, 12260−12269.

(9) Mahadevan, D., Powis, G., Mash, E. A., George, B., Gokhale, V. M., Zhang, S., Shakalya, K., Du-Cuny, L., Berggren, M., Ali, M. A., Jana, U., Ihle, N., Moses, S., Franklin, C., Narayan, S., Shirahatti, N., and Meuillet, E. J. (2008) Discovery of a novel class of AKT pleckstrin homology domain inhibitors. *Mol. Cancer Ther. 7*, 2621−2632.

(10) Moses, S. A., Ali, M. A., Zuohe, S., Du-Cuny, L., Zhou, L. L., Lemos, R., Ihle, N., Skillman, A. G., Zhang, S., Mash, E. A., Powis, G., and Meiullet, E. J. (2009) In vitro and in vivo activity of novel small-molecule inhibitors targeting the pleckstrin homology domain of protein kinase B/AKT. *Cancer Res. 69*, 5073−5081.

(11) Meuillet, E. J., Zuohe, S., Lemos, R., Ihle, N., Kingston, J., Watkins, R., Moses, S. A., Zhang, S., Du-Cuny, L., Herbst, R., Jacoby, J. J., Zhou, L. L., Ahad, A. M., Mash, E. A., Kirkpatrick, D. L., and Powis, G. (2010) Molecular pharmacology and antitumor activity of PHT-427, a novel Akt/phosphatidylinositide-dependent protein kinase 1 pleckstrin homology domain inhibitor. *Mol. Cancer Ther. 9*, 706−717.

(12) Barratt, G., Saint-Pierre-Chazalet, M., and Loiseau, P. M. (2009) Cellular transport and lipid interactions of miltefosine. *Curr. Drug Metab. 10*, 247−255.

(13) Moreira, R. A., Mendanha, S. A., Hansen, D., and Alonso, A. (2013) Interaction of miltefosine with the lipid components of the erythrocyte membrane. *J. Pharm. Sci. 102*, 1661−1669.

(14) Carrasco, M. P., Jiménez-López, J. M., Ríos-Marco, P., Segovia, J. L., and Marco, C. (2010) Disruption of cellular cholesterol transport and homeostasis as a novel mechanism of action of membrane-targeted alkylphospholipid analogues. *Br. J. Pharmacol. 160*, 355−366.

(15) Redfield, A. G. (2012) High-resolution NMR field-cycling device for full-range relaxation and structural studies of biopolymers on a shared commercial instrument. *J. Biomol. NMR 52*, 159−177.

(16) Roberts, M. F., and Redfield, A. G. (2004) High-resolution ^{31}P field cycling NMR as a probe of phospholipid dynamics. *J. Am. Chem. Soc. 126*, 13765−13777.

(17) Roberts, M. F., and Redfield, A. G. (2004) Phospholipid bilayer surface configuration probed quantitatively by ^{31}P field-cycling NMR. *Proc. Natl. Acad. Sci. U.S.A. 101*, 17066−17071.

(18) Pu, M., Feng, J., Redfield, A. G., and Roberts, M. F. (2009) Enzymology with a spin-labeled phospholipase C: Soluble substrate binding by ^{31}P NMR from 0.005 to 11.7 T. *Biochemistry 48*, 8282−8284.

(19) Pu, M., Orr, A., Redfield, A. G., and Roberts, M. F. (2010) Defining specific lipid binding sites for a peripheral membrane protein

in situ using subtesla field-cycling NMR. *J. Biol. Chem. 285*, 26916−26922.
(20) Cheng, J., Goldstein, R., Gershenson, A., Stec, B., and Roberts, M. F. (2013) The cation-π box is a specific phosphatidylcholine membrane targeting motif. *J. Biol. Chem. 288*, 14863−14873.
(21) Gasteiger, E., Hoogland, C., Gattiker, A., Duvaud, S., Wilkins, M. R., Appel, R. D., and Bairoch, A. (2005) in *The Proteomics Protocols Handbook* (Walker, J. M., Ed.) pp 571−607, Humana Press, New York.
(22) Chang, T., Wang, R., Olson, D. J., Mousseau, D. D., Ross, A. R., and Wu, L. (2011) Modification of Akt1 by methylglyoxal promotes the proliferation of vascular sooth muscle cells. *FASEB J. 25*, 1746−1757.
(23) Koojman, E. E., King, K. E., Gangoda, M., and Gericke, A. (2009) Ionization properties of phosphatidylinositol polyphosphates in mixed model membranes. *Biochemistry 48*, 9360−9371.
(24) Martin, J.-B., Foray, M.-F., Klein, G., and Satre, M. (1987) Identification of inositol hexakisphosphate in ^{31}P-NMR spectra of *Dictyostelium discoideum* amoebae. Relevance to intracellular pH determination. *Biochim. Biophys. Acta 931*, 16−25.
(25) Pochapsky, T. C., and Pochapsky, S. S. (2007) *NMR for Physical and Biological Sciences*, 1st ed., Taylor and Francis, Garland Science, New York.
(26) Emsley, P., and Cowtan, K. (2004) Coot: Model-building tools for molecular graphics. *Acta Crystallogr. D60*, 2126−2132.
(27) *The PyMOL Molecular Graphics System*, version 1.5.0.4 (2012) Schrödinger, LLC, Portland, OR.
(28) Schüttelkopf, A. W., and van Aalten, D. M. F. (2004) PRODRG: A tool for high-throughput crystallography of protein-ligand complexes. *Acta Crystallogr. D60*, 1355−1363.
(29) Grosdidier, A., Zoete, V., and Michielin, O. (2011) SwissDock, a protein-small molecule docking web service based on EADock DSS. *Nucleic Acids Res. 39*, W270−W277.
(30) Ivanov, D., Bachovchin, W. W., and Redfield, A. G. (2002) Boron-11 pure quadrupole resonance investigation of peptide boronic acid inhibitors bound to α-lytic protease. *Biochemistry 41*, 1587−1590.
(31) Wang, Y. K., Chen, W., Blair, D., Pu, M., Xu, Y., Miller, S. J., Redfield, A. G., Chiles, T. C., and Roberts, M. F. (2008) Insights into the structural specificity of the cytotoxicity of 3-deoxyphosphatidylinositols. *J. Am. Chem. Soc. 130*, 7746−7755.
(32) Berg, H. C. (1993) *Random Walks in Biology*, Princeton University Press, Princeton, NJ.
(33) Lukác, M., Pisárcik, M., Lacko, I., and Devínsky, F. (2010) Surface-active properties of nitrogen heterocyclic and dialkylamino derivates of hexadecylphosphocholine and cetyltrimethylammonium bromide. *J. Colloid Interface Sci. 347*, 233−240.
(34) Pilling, C., Landgraf, K. E., and Falke, J. J. (2011) The GRP1 PH domain, like the Akt1 PH domain, possesses a sentry glutamate residue essential for specific targeting to plasma membrane PI(3,4,5)P_3. *Biochemistry 50*, 9845−9856.
(35) Gills, J. J., Zhang, C., Abu-Asab, M. S., Castillo, S. S., Marceau, C., LoPiccolo, J., Kozikowski, A. P., Tsokos, M., Goldkorn, T., and Dennis, P. A. (2012) Ceramide mediates nanovesicle shedding and cell death in response to phosphatidylinositol ether lipid analogs and perifosine. *Cell Death Dis. 3*, e340.
(36) Rakotomanga, M., Loiseau, P. M., and Saint-Pierre-Chazalet, M. (2004) Hexadecylphosphocholine interaction with lipid monolayers. *Biochim. Biophys. Acta 1661*, 212−216.
(37) Wu, W., Voegtli, W. C., Sturgis, H. L., Dizon, F. P., Vigers, G. P., and Brandhuber, B. J. (2010) Crystal structure of human AKT1 with an allosteric inhibitor reveals a new mode of kinase inhibition. *PLoS One 5*, e12913.
(38) Clarkson, M. w., Lei, M., Eisenmesser, E. A., Labeikovsky, W., Redfield, A. G., and Kern, D. (2009) Mesodynamics in the SARS nucleocapsid measured by NMR field cycling. *J. Biomol. NMR 45*, 217−225.
(39) Charlier, C., Khan, S. N., Marquardsen, T., Pelupessy, P., Reiss, V., Sakellariou, D., Bodenhausen, G., Engelke, F., and Ferrage, F. (2013) Nanosecond time scale motions in proteins revealed by high-resolution NMR relaxometry. *J. Am. Chem. Soc. 135*, 18665−18672.